

NARROWBAND SOURCE LOCALIZATION IN AN UNKNOWN REVERBERANT ENVIRONMENT USING WAVEFIELD SPARSE DECOMPOSITION

Gilles Chardon, Laurent Daudet

Institut Langevin, CNRS UMR 7587, UPMC, Univ. Paris Diderot, ESPCI, 75005 Paris, France

ABSTRACT

We propose a method for narrowband localization of sources in an unknown reverberant field. A sparse model for the wavefield is introduced, derived from the physical equations. We compare two localization algorithms that take advantage on the structured sparsity naturally present into the model : a greedy iterative scheme, and an ℓ_1 minimization method. Both methods are validated in 2D on numerical simulations, and on experimental data with a chaotic-shaped plate. These results, robust with respect to the specific sampling of the field and to noise, show that this approach may be an interesting alternative to traditional approaches of source localization, when a large number of narrowband sensors are deployed.

Index Terms— source localization, sparsity, acoustic waves, plate vibrations, room acoustics.

1. INTRODUCTION

Numerous methods for source localization in a vibrating medium have been developed, with various models and algorithms. Most of them assume either a free field propagation [1], or, in the case of an enclosed space with strong reverberation, specific prior knowledge about the propagation and reverberation, for instance a pre-measured database of impulse responses [2].

The method introduced here deals with the case of a possibly strong, but unknown, reverberant field. It is based on a sparse model of the wavefield within an enclosed space, directly derived from the partial differential equation governing the variations of the pressure field. Apart from homogeneity and isotropy, we do not assume any prior knowledge on the propagation medium. In particular, the dispersion of the medium and its boundary conditions are left unspecified, making this method relevant for a wide range of cases, such as membranes, plates or rooms. From a number of point measurements at a single frequency, sources can be localized even in the presence of a strong reverberant field, or additional sources outside the region of interest. In these cases, standard methods such as beamforming, MUSIC, time reversal, etc., would not be appropriate. The price to pay for this performance is a high number of point measurements (i.e., sensors) around the sources in the space of interest, significantly larger than for traditional methods. This number is, however, smaller than the number of sensors required by the sampling theorem to unambiguously measure the wavefield. Note also that we only consider here measurements at a single frequency: the extension to wideband measurements, that would require more sophisticated structured sparsity models, is left for further research.

{gilles.chardon, laurent.daudet}@espci.fr

This work was partly funded by the Agence Nationale de la Recherche (ANR), project ECHANGE (ANR-08-EMER-006). LD is on a joint affiliation between Univ. Paris Diderot and Institut Universitaire de France.

Section 2 of this paper introduces the sparse model used to describe the impulse responses. Two localization algorithms based on this model are described in section 3. Simulated as well as experimental results are given in section 4 and 5, respectively. Section 6 concludes the paper.

2. SPARSE MODELING OF WAVEFIELDS

Let us start, for the sake of simplicity, with the case of the acoustic pressure within a room. The pressure field $p(\mathbf{x}, t)$ satisfies the wave equation:

$$\begin{cases} \Delta p - \frac{1}{c^2} \frac{\partial^2 p}{\partial t^2} = s(\mathbf{x}, t) \\ \text{boundary conditions} \end{cases}$$

with c being the wave velocity and $s(\mathbf{x}, t)$ the sources. Here, the boundary conditions do not have to be explicitly given, but classical examples would be Dirichlet, Neumann, or impedance conditions. The source term is assumed to be the sum of few punctual sources located at points \mathbf{x}_j :

$$s(\mathbf{x}, t) = \sum_{j=1}^S s_j(t) \delta_{\mathbf{x}_j}(\mathbf{x})$$

with $\delta_{\mathbf{x}_j}$ a Dirac at point \mathbf{x}_j .

In the frequency domain, the wave equation becomes the Helmholtz equation: for all ω , the Fourier transform $\hat{p}(\mathbf{x}, \omega)$ of the pressure satisfies

$$\begin{cases} \Delta \hat{p} + k^2 \hat{p} = \hat{s} \\ \text{boundary conditions} \end{cases}$$

where the wavenumber k equals ω/c . The source term is here

$$\hat{s}(\mathbf{x}, \omega) = \sum_{j=1}^S \hat{s}_j(\omega) \delta_{\mathbf{x}_j}(\mathbf{x}).$$

The first step towards a sparse model of the room response is to decompose it as the sum of a particular solution of the equation without the boundary conditions, and a solution of the homogeneous equation with adequate boundary conditions. Physically, these two components represent the direct contribution of the sources and the diffuse field, respectively.

The contribution of a source at point \mathbf{x}_0 is an Hankel function of order 0: $h_0^{(1)}(k|\mathbf{x} - \mathbf{x}_0|) = j_0(k|\mathbf{x} - \mathbf{x}_0|) + iy_0(k|\mathbf{x} - \mathbf{x}_0|)$. The first kind Bessel function j_0 will here be included in the homogeneous component p_0 . The particular solution p_s , representing the direct contribution of the sources, can thus be chosen as a sum of Bessel functions of the second kind y_0 , at order 0:

$$p_s(\mathbf{x}, \omega) = \frac{k}{4\pi} \sum_{j=1}^S \hat{s}_j(\omega) y_0(k|\mathbf{x} - \mathbf{x}_j|)$$

The homogeneous part p_0 , for the diffuse field, is solution of the homogeneous Helmholtz equation. It also satisfies some boundary conditions that depend on the boundary conditions of the total field, as well as on the field generated by possibly other sources outside of the considered domain. As this field is unknown, the boundary conditions satisfied by the diffuse field are unknown. However, independently of the boundary conditions, a solution of the homogeneous Helmholtz equation can be approximated by a sum of L plane waves $e_l(\mathbf{x}) = \exp(i\mathbf{k}_l \cdot \mathbf{x})$ where the wave vectors \mathbf{k}_l have polar coordinates $(r, \theta) = (k, 2\pi l/L)$ [3]:

$$p_0 \approx \sum_{l=1}^L \alpha_l e_l(x)$$

Note that the number L of plane waves needed for a good approximation of \hat{p}_0 is significantly less than the overall dimensionality of the problem, i.e. the number of samples needed by the sampling theorem or the size of the discretization for standard numerical schemes like finite differences or finite elements. Indeed, while the size of standard discretization schemes scales like the square of the product of the wave number by the diameter of the domain of interest, plane wave description of the field needs a number of components proportional to this product.

Finally, our sparse model for solutions of the Helmholtz equation with punctual sources writes:

$$\hat{p} \approx \sum_{l=1}^L \alpha_l e_l(\mathbf{x}) + \sum_{j=1}^S \hat{s}_j(\omega) y_0(k||\mathbf{x} - \mathbf{x}_j||).$$

with unknowns α_l , the coefficients of the decomposition of the diffuse field, $\hat{s}_j(\omega)$ and \mathbf{x}_j , the amplitude and positions of the sources, to be determined. In practice, the diffuse field (the first term) can be much larger than the source field (the second term) containing the informations to be retrieved. It should be emphasized that the sparsity in this wavefield decomposition is of very different nature in each of its two terms: in the first term, sparsity arises from the structure of the approximation subspace, chosen as the span of plane waves restricted to sharing the same wavenumber. In contrast, sparsity in the second term has the more standard form, where we assume that only few source amplitudes $\hat{s}_j(\omega)$ are non-zero.

3. ALGORITHMS

A dictionary \mathbf{D} is created from this model by quantizing the locations of candidate sources on a regular grid, at points \mathbf{y}_j . The field is measured at M points \mathbf{x}_m . The dictionary \mathbf{D} is composed of the concatenation of two sub-dictionaries:

- a dictionary of plane waves \mathbf{W} , sampled at locations \mathbf{x}_m . Its (m, l) term is $w_{ml} = e_l(\mathbf{x}_m)$,
- a dictionary of source terms \mathbf{S} at candidate locations \mathbf{y}_j , sampled at the same locations \mathbf{x}_m . Its (m, j) term is $s_{mj} = y_0(k||\mathbf{y}_j - \mathbf{x}_m||)$.

The sampled wavefield \mathbf{p} then writes

$$\mathbf{p} = \mathbf{W}\boldsymbol{\alpha} + \mathbf{S}\boldsymbol{\beta}$$

where no priors are assumed on the coefficients of the plane waves α_l , while the coefficients of the source terms β_j are assumed sparse: the size of the support of $\boldsymbol{\beta}$ is the number of sources.

As the sparse model used to describe the impulse responses is not standard, specific algorithms have to be designed. Here, we propose two simple modifications of standard sparse regression algorithms: the first one is based on Orthogonal Matching Pursuit (OMP) [4], the second on a group sparsity version of Basis Pursuit [5].

3.1. Greedy source localization algorithm

OMP identifies the sources iteratively, by correlating the measurements with a dictionary of sources. Here, a direct application of this algorithm would fail, as the correlation between the sources and the dictionary would be masked by the correlations with the diffuse field. The initialization step of the modified algorithm is then to “clean” out this diffuse field. As shown before, this diffuse field is approximated by a space spanned by a set of plane waves. Hence, cleaning the diffuse field is achieved by projecting the measurements on the orthogonal complement of the plane wave space. Now, correlations with this cleaned field allow the identification of the first source. The original field is then projected on the orthogonal complement of the space by the plane waves and the first identified source. Correlations with this field identifies the second source, and so on.

Algorithm 1 Greedy source localization algorithm

Input: measurements \mathbf{p} , number of sources n , plane waves dictionary \mathbf{W} , source atoms \mathbf{s}_y

Output: estimated positions of the sources \mathbf{y}_j

```

 $\mathbf{p}_s \leftarrow \mathbf{W}\mathbf{W}^\dagger \mathbf{p}$ 
for  $j = 1$  to  $n$  do
   $\mathbf{y}_j \leftarrow \arg \max_y |\langle \mathbf{s}_y, \mathbf{p}_s \rangle|$ 
   $\mathbf{W} \leftarrow (\mathbf{W} | \mathbf{s}_{\mathbf{y}_j})$ 
   $\mathbf{p}_s \leftarrow \mathbf{W}\mathbf{W}^\dagger \mathbf{p}$ 
end for

```

3.2. Group Basis Pursuit

The second algorithm is based on the Basis Pursuit framework: sparse signals are recovered via minimization of their ℓ_1 norm with constraints modeling the measurements. More complex sparsity models can be recovered via minimization of structured norms [6].

Here, the minimisation problem to be solved is

$$(\hat{\boldsymbol{\alpha}}, \hat{\boldsymbol{\beta}}) = \min_{\boldsymbol{\alpha}, \boldsymbol{\beta}} ||\boldsymbol{\alpha}||_2 + ||\boldsymbol{\beta}||_1 \quad \text{s.t.} \quad ||\mathbf{W}\boldsymbol{\alpha} + \mathbf{S}\boldsymbol{\beta} - \mathbf{p}|| < \epsilon$$

where ϵ is the expected amount of noise in the measurements. The ℓ_2 norm on the $\boldsymbol{\alpha}$ coefficients indicate that this set of coefficients does not have to be sparse: sparsity of the diffuse field arises from the fact that only plane waves with wave vector \mathbf{k}_j with modulus k are allowed, but all coefficients can be non-zero. After minimization, the few non-zero coefficients of $\boldsymbol{\beta}$ indicate the location and amplitude of the sources.

4. NUMERICAL SIMULATIONS

The algorithm is first tested on simulated data. For the ease of implementation, and better visualization, these simulations are run in 2D. Solutions of the Helmholtz equation for a square membrane, with 2 sources, are computed using FreeFem++, a finite element solver [7].

Greedy algorithm: The simulated field is shown on fig. 1(a), and fig. 1(b) displays the 121 measurement points, taken at random

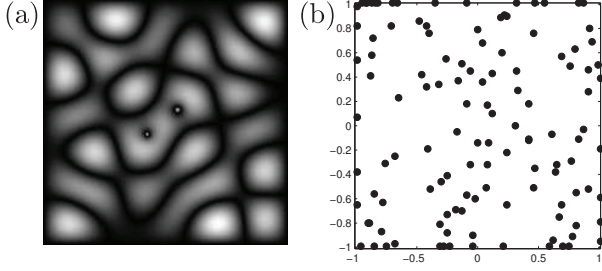


Fig. 1. Numerical simulations : (a) Modulus of the simulated field (b) Position of samples used for the localization

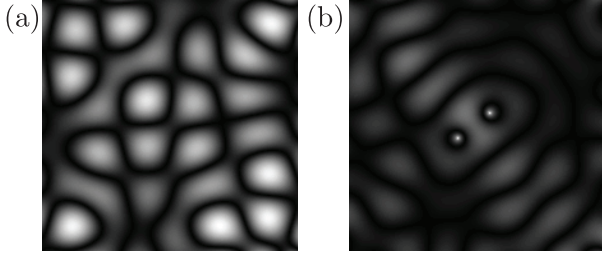


Fig. 2. Numerical simulations : Decomposition of the measurements as (a) diffuse component p_0 and (b) source component p_s

within the surface of interest and on its contour. The wavefield decomposition as a diffuse field (projection on the span of the plane waves), plus a source field (estimated as the difference between original and diffuse field), is shown on fig. 2. As shown on fig. 3, correlating the samples with the source atoms before this decomposition gives no useful informations about the position of the sources. Actually, the correlation with the total field is the sum of the correlation with the diffuse field and the source field:

$$\langle \mathbf{s}_y, \mathbf{p} \rangle = \langle \mathbf{s}_y, \mathbf{p}_0 \rangle + \langle \mathbf{s}_y, \mathbf{p}_s \rangle$$

The diffuse field \mathbf{p}_0 being significantly larger than the source field \mathbf{p}_s , the correlations we are interested in are masked by the large correlations with the diffuse field. However, after projection on the orthogonal complement of the plane wave space, the localization information enclosed in the field becomes more visible. The correlations computed at the first step of OMP allow the identification of the first source. The second source is then identified at the second iteration: figure 3 shows the correlations at the second step, and the estimated positions of the sources, which are near the true positions.

Group basis pursuit: Here again, application of Basis Pursuit using the free field model fails as can be seen on fig. 4(a): artifacts on the border of the domain appear. This can be interpreted as a tentative by Basis Pursuit to explain the diffuse field as a sum of source terms placed outside of the domain, as would be done by the Method of Fundamental Solutions [8]. Using the Group Basis Pursuit as implemented in the spg11 toolbox [9] [10], and the modified objective function, we obtain a correct estimation of the sources position, as seen on fig. 4(b) without artifacts.

5. EXPERIMENTAL RESULTS

Finally, we test our localization method on real experimental data, with a single source on a metallic plate. The experimental setup is

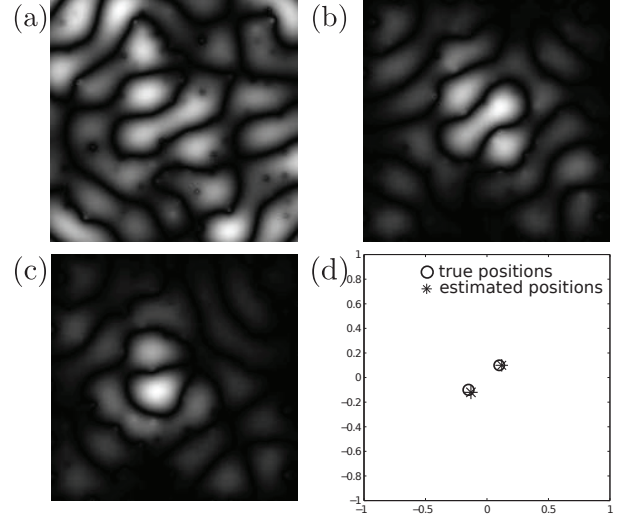


Fig. 3. Numerical simulations : Correlations at the first step of the greedy algorithm (a) before and (b) after the projection. (c) Correlations at the second step. (d) Estimated source positions.

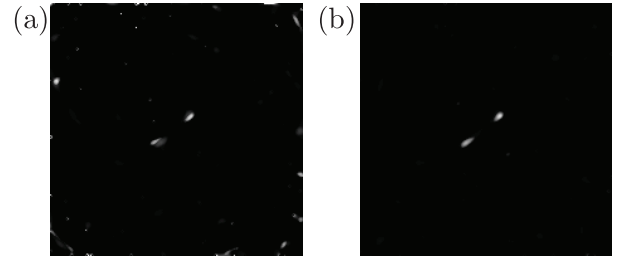


Fig. 4. Numerical simulations : Sources estimated by (a) basis pursuit with sources dictionary (b) group basis pursuit with plane waves and sources dictionary

pictured on fig 5: the plate is excited by a piezoelectric transducer (PZT), and its normal displacement is measured by a laser vibrometer. The behavior of this displacement w is governed, in the case of thin plates, by the Kirchhoff-Love equation:

$$D\Delta^2 w + 2\rho h \frac{\partial^2 w}{\partial t^2} = f$$

where D is the bending stiffness of the plate, ρ its density, h its thickness and f the normal force applied to the plate. As shown in [11], approximation of the solutions of the plate equation without right-hand term would need propagative ($e^{ik \cdot x}$) and exponential ($e^{k \cdot x}$) waves. However, the domain of interest being far from the boundaries, the latter can be neglected. Sources terms are then the sum of a second kind Bessel function and a second kind modified Bessel function, the latter being neglected here.

As the dispersion relation of the plate is here not known, a prior estimation of the correct wave number is necessary. The estimation is done using the procedure described in [11]. As the source field is, again, weak compared to the diffuse field, the estimation of the wave number is not perturbed by the presence of sources.

Remarkably, as observed in [11], the field can be sampled on a regular grid with a sub-Nyquist step (a period slightly larger than the half wave-length), without any significant effect on the estimation of

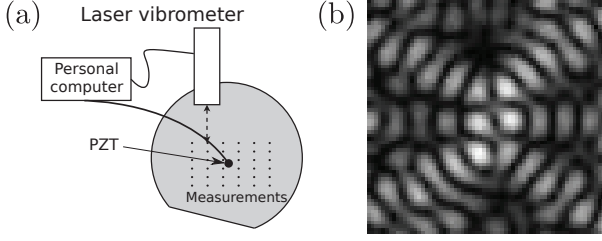


Fig. 5. (a) Experimental setup (b) Amplitude of the field measured at frequency $f = 30631$ Hz on a 4mm sampling grid.

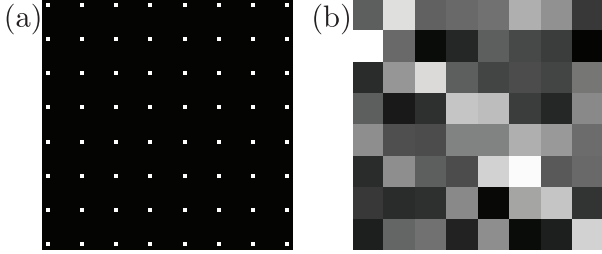


Fig. 6. (a) Uniform sub-Nyquist sampling used for localization (b) Amplitude of the corresponding measured subsampled field

the wavenumber nor the diffuse field. Here, we used a square grid of 64 samples, with a step size of 32 mm. At the frequency $f = 30631$ Hz, the estimated wavelength is 49.4 mm (the half wavelength is indeed smaller than the sampling step). The samples used as well as the amplitude of the measured signal are drawn on fig. 6.

Greedy algorithm: Correlations for the first step of OMP (the only step in this 1-source case) are shown on fig. 7, before and after projection. Source localization fails before projection, while after, the source can be clearly localized near the center of the domain.

Group basis pursuit: Source estimation was performed with plain Basis Pursuit (source-only dictionary of Bessel functions) and Group Basis Pursuit (full dictionary, with plane waves and sources). Estimated source locations are shown on fig. 8 (a) and (b), respectively. Again, the full dictionary is required for accurate source localization.

6. CONCLUSION

We introduced a new source localization framework working in an unknown reverberant environment. While it has here been formulated in a narrowband situation, generalization to wideband signals would lead to joint sparsity across frequencies. Similarly, the method can be extended to directional sources with the use of a larger source dictionary and group sparsity.

Although the algorithms proposed here show good performance both in numerical tests and on real measurements, there are still a number of open issues. For instance, the minimum number of sensors and their optimal positions are still open questions.

Finally, we used here the standard sparsity-at-synthesis viewpoint. Further work will compare these results to the ones obtained via newer sparsity-at-analysis approaches.

7. ACKNOWLEDGEMENTS

The authors thank A. Leblanc for the experimental measurements.

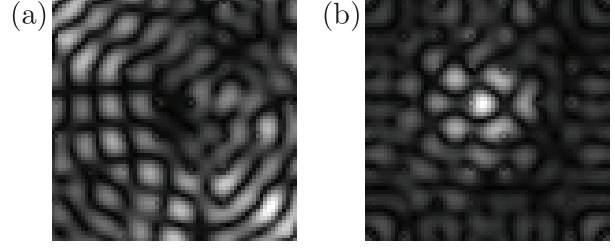


Fig. 7. Correlations at the first step of the greedy algorithm (a) before and (b) after the projection, on the experimental data.

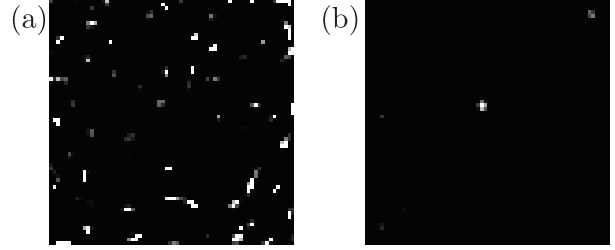


Fig. 8. Source position and amplitude estimated by (a) basis pursuit (source-only dictionary) (b) group basis pursuit (full dictionary)

8. REFERENCES

- [1] D. Malioutov, M. Cetin, and A. S. Willsky, "A sparse signal reconstruction perspective for source localization with sensor arrays," *IEEE Trans. Sig. Proc.*, vol. 53, no. 8, 2005.
- [2] R.-K. Ing, N. Quieffin, S. Catheline, and M. Fink, "In solid localization of finger impacts using acoustic time-reversal process," *Applied Physics Letters*, vol. 87, no. 20, 2005.
- [3] A. Moiola, R. Hiptmair, and I. Perugia, "Plane wave approximation of homogeneous Helmholtz solutions," *Zeitschrift für Angewandte Mathematik und Physik*, vol. 62, 2011.
- [4] J.A. Tropp and A.C. Gilbert, "Signal recovery from random measurements via orthogonal matching pursuit," *IEEE Trans. Inf. Th.*, vol. 53, no. 12, 2007.
- [5] S.S. Chen, D.L. Donoho, and M.A. Saunders, "Atomic decomposition by basis pursuit," *SIAM J. Sci. Comp.*, vol. 20, 1998.
- [6] F. Bach, "Structured sparsity-inducing norms through submodular functions," in *Advances in Neural Information Processing Systems*, Vancouver, Canada, 2010, p. NIPS.
- [7] O. Pironneau, F. Hecht, Le Hyaric A., and Morice J., "FreeFem++," <http://www.freefem.org/ff++>.
- [8] G. Fairweather and A. Karageorghis, "The method of fundamental solutions for elliptic boundary value problems," *Adv. Comp. Math.*, vol. 9, 1998.
- [9] E. van den Berg and M. P. Friedlander, "SPGL1: A solver for large-scale sparse reconstruction," June 2007, <http://www.cs.ubc.ca/labs/scl/spgl1>.
- [10] E. van den Berg and M. P. Friedlander, "Probing the Pareto frontier for basis pursuit solutions," *SIAM Journ. Sc. Comp.*, vol. 31, no. 2, 2008.
- [11] G. Chardon, A. Leblanc, and L. Daudet, "Plate impulse response spatial interpolation with sub-Nyquist sampling," *Journ. Sound Vibration*, vol. 330, no. 23, 2011.